THE JOURNAL OF PHYSICAL CHEMISTRY B

Article

Computational Investigation of Interaction between Nanoparticles and Membranes: Hydrophobic/Hydrophilic Effect

Yang Li, Xin Chen, and Ning Gu

J. Phys. Chem. B, **2008**, 112 (51), 16647-16653 • DOI: 10.1021/jp8051906 • Publication Date (Web): 25 November 2008

Computational Investigation of Interaction between Nanoparticles and Membranes: Hydrophobic/Hydrophilic Effect

Yang Li, Xin Chen, and Ning Gu*

State Key Laboratory of Bioelectronics and Jiangsu Laboratory for Biomaterials and Devices, Southeast University, Nanjing, 210096, P. R. China

Received: June 12, 2008; Revised Manuscript Received: September 29, 2008

Understanding the interactions of nanoparticles (NPs) with biological system, especially interactions with cell membranes, is critical for the rational design of nanocarrier agents and drug delivery systems. Here, we have performed coarse-grained molecular dynamics simulations aimed at the effect of hydrophilic/hydrophobic properties of nanoparticles on the interaction with cell membranes (dipalmitoylphosphatidylcholine or DPPC bilayer). Two kinds of nanoparticles (hydrophobic and semihydrophilic) are modeled in the simulation. The results indicate that a hydrophobic nanoparticle can result in the inclusion into the bilayer, whereas a semihydrophilic nanoparticle is only found to adsorb into the membrane. For different system free energy profiles have been calculated to elucidate those phenomena. For the semihydrophilic nanoparticle case, we also discuss the potential substantial energy barrier of particle wrapping, implicating that the endocytosis-like mechanism is an energy-mediated process. The landscapes of the membrane fluctuation in the transitions imply that the deformation of the lipid bilayer induced by the addition of NPs is short-range, and the rearrangement of lipid molecules plays a significant role for morphological variations of NP-containing lipid membrane patches. These results show that the surface hydrophobicity can result in different response mechanisms of NP−biomembrane interactions.

I. Introduction

The biologic effects of nanoparticles (NPs) are dependent on their unique properties, e.g., size, hydrophobicity, chemical composition, shape, surface charge density, and aggregation. These parameters can affect cellular uptake, protein binding, and translocation from portal of entry to the target site, etc.[1,2] Therefore, a basic understanding of the interactions of nanoparticles with biological systems, especially with cell membrane, becomes a crucial task in determining the cytotoxicity of nanoparticles as well as their potential application as drug delivery vehicles or therapeutic agents.[3,4]

Hydrophobicity is a very important factor in the interaction of nanomaterials with the biomembrane. Assembly behaviors of nanoparticles can be driven by hydrophobic/hydrophilic (or interfacial) effort.[5−7] For the design of drug delivery system, modifying the surface hydrophobic/hydrophilic effects of nanoparticles can guide the location of the NPs on the surface or within a specific compartment of the vesicle.[8] From the perspective of NP−biomembrane interaction, many recent researches, demonstrating different response mechanisms of the lipid bilayer induced by the hydrophobicity of NPs, have been reported in experiments[9−12] and in computer simulations.[13−16] When interacting with cells, some flexible macromolecules, such as protein[11] and polymer,[12] can penetrate the biomembrane via changing their configurations driven by the hydrophobicity. Hong et al. have reported that uncharged ("hydrophobic") PAMAM dendrimers absorb to the existing supported lipid bilayers, while the charged ones can make a hole on the membrane.[9] These experiments have been explained by computer simulations respectively based on self-consistent field/density functional theory[14] and molecular dynamics (MD) simulations.[17] Qiao et al. have reported different translocation behaviors of fullerene molecules across a lipid bilayer due to the surface hydrophobicity of fullerene NPs.[15] Whereas a hydrophobic fullerene molecule can penetrate the bilayer, its derivatives of hydrophilic surface functionalization only adsorb to the bilayer. These existing results show that the hydrophobicity effect can regulate the NPs either adsorbing onto the membrane or embedding into the inner of the bilayer. Besides the hydrophobicity effect, the size of nanoparticles also plays an important role during the interaction.[10,14,18] No matter inclusion or adhesion, larger nanoparticles may result in different morphological changes of the biomembrane from those induced by smaller ones.[10,19] According to the conclusion of ref 14, there seems to be a size effect in the NP−biomembrane interaction where the critical size is ∼10 nm. Nonetheless, apart from only a few papers, describing the strong correlation between permeability of trans-membrane and the solubility of solute molecules[13] or some small nanoparticles,[14,15,17] the response mechanisms of biomembranes associated with the hydrophobicity property of nanoparticles, whose diameter is larger than the thickness of the membrane, have not been investigated systematically. Miha et al. have described the bending elasticity of the biomembrane due to the inclusion.[19,20] The adsorption and wrap of nanoparticles by a fluid membrane have been reported by Deserno.[21] In spite of a large NP used in the simulations, both of their results, which are based on the frameworks at the mean-field level, cannot reveal the microscopic kinetics of the process at the molecular level.

The present paper focuses on demonstrating how the hydrophobicity effects of nanoparticles can influence the interactions with the lipid bilayer via molecular dynamics simulations. Two kinds of NPs, hydrophobic and semihydrophilic, are considered in our simulations. And the diameter of NPs is ∼10 nm, larger than the normal thickness of the bilayers. Whereas a hydro-

* Corresponding author: Fax +86-25-83274960; Tel +86-25-83792576; e-mail guning@seu.edu.cn.

10.1021/jp8051906 CCC: $40.75
Published on Web 11/25/2008

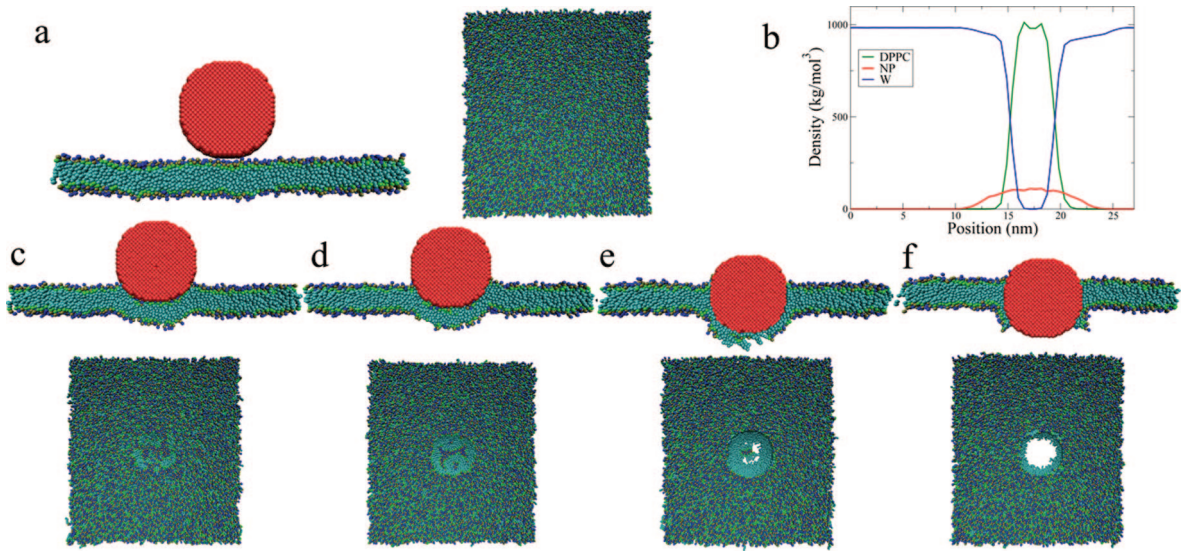

Figure 1. Trajectory snapshots of hydrophobic NP simulation in stereo views: (a) the initial configuration of the simulation system, (b) density profiles for different components of the final configuration, (c) the NP adsorbing on the surface of the bilayer, (d) the adsorption of the NP disturbing the headgroup of the lipid bilayer, (e) the embedding behavior of the NP inducing the pore formation on the bilayer, (f) the final equilibrium stage, the NP staying at the embedded pore of the lipid bilayer. A red bead cluster represents the nanoparticle; blue beads and green beads represent the DPPC bilayer. The explicit water molecules are omitted for clarity. The images are created with VMD.[38]

phobic nanoparticle can result in the inclusion into the bilayer, a semihydrophilic nanoparticle is only observed to adsorb into the membrane. For different systems some thermodynamics parameters have been obtained to elucidate the differences. Free energy profiles can provide information on the probability of the NP penetrations through the membrane. And the landscapes of the membrane fluctuation in the transition reflect a perturbation effect of NPs on the membrane. These results show that the surface hydrophobicity can result in different response mechanisms of NP−biomembrane interactions.

II. Methods

Atomistic simulations reveal maximum details but are restricted to small length and time scales. In view of the relatively large length and time scales of the biological phenomenon in our simulations, a coarse-grained (CG) lipid model has been employed directly for its ability to reproduce experimental properties of various lipid assemblies.[22] The CG model includes four main types of interaction sites: polar (P), nonpolar (N), apolar (C), and charged (Q). For particles of type N and Q four subtypes (0, d, a, and da) are further distinguished to allow fine-tuning of the Lennard-Jones (LJ) interactions, reflecting hydrogen-bonding capabilities. Force field parameters and further information on the CG model are available in the Supporting Information, SI_1. A CG DPPC molecule is comprised of 12 beads. The headgroup includes two charged beads: one bead (Q0) for the choline (NC3) with one unit of positive charge and one bead (Qa) for the phosphate (PO4) with one unit of negative charge. Two nonpolar beads (Na) compose the glycerol ester backbone (GL). Each of two tails (Ctail) consists of four apolar beads (C), of which each methylene unit is mapped into a tail bead. For a CG water (W), each bead (P) represents four water molecules. A solid, nearly spherical nanoparticle is modeled as a face-centered-cubic lattice, consisting of 15 635 beads, whose diameter is ∼10 nm. We use different types of beads to represent hydrophobic/hydrophilic properties, where the hydrophobic nanoparticle is consisted of the apolar beads (C) and the semihydrophilic nanoparticle of the nonpolar beads (Nd). Because the aim of our study is not to investigate the effect of surface charges on cellular uptake, we do not model surface charges of particles here. The beads comprising a single nanoparticle are constrained to move as a rigid body. We have verified that water and lipid beads do not penetrate the interior of the particle under these conditions (see Supporting Information, SI_2).

A cubic periodic box with cell dimensions of 43.4 × 47.7 × 23.6 nm^3 is constructed at the origin, containing 389 547 CG water molecules and a patch of CG biomembrane, which consists of 6272 CG DPPC molecules. After energy minimization, equilibration runs have been performed for 20 ns with a time step of 40 fs. The final equilibrium configuration is used as the starting state for the next simulation with nanoparticles participation.

An equilibrated nanoparticle is then added into the system. The final configuration includes a nanoparticle, lipid bilayer, and water molecules in a box with dimensions of 43.1 × 46.7 × 26.7 nm^3, shown in Figure 1a. To facilitate the following discussion, we define the midplane of the lipid bilayer as the $X-Y$ plane and introduce the Z axis which is perpendicular to the bilayer surface. After energy minimization, the nanoparticle is position-restrained with a force constant of 1000 kJ mol^{-1} nm^{-2}, and a gradual pre-equilibration run of 5 ns has been performed to remove incorrect overlaps and ensure that all degrees of freedom are adjusted as much as possible in the initial configuration. In full equilibration process, considering little contributions of $X-Y$ dimension movement to the rigid nanoparticle across through the bilayer, the nanoparticle is harmonically restrained, and the constraints with a force constant of 1000 kJ mol^{-1} nm^{-2} are applied through resetting the $X-Y$ coordinates of the nanoparticle at every time step to their reference positions. The reference positions equal the initial positions of the inserted nanoparticle except for small fluctuations. The full equilibration runs have been performed for 20 ns in the hydrophobic NP−membrane simulation and for 15 ns in the semihydrophilic NP−membrane simulation.

For all simulations, a Berendsen thermostat/barostat[23] is used to maintain a constant temperature of 323 K and a constant pressure of 1 atm in the NPT ensemble. A cutoff of 1.2 nm is

used for van der Waals interactions, and the Lennard-Jones potential is smoothly shifted to zero between 0.9 and 1.2 nm to reduce the cutoff noise. For electrostatic interaction, the Coulombic potential, with a cutoff of 1.2 nm, is also smoothly shifted to zero from 0 to 1.2 nm.[22] All the simulations have been performed with the GROMACS 3.3.2 simulation package.[24]

III. Results and Discussion

Simulations of Hydrophobic Nanoparticles. A striking effect of membrane disruption under the NP invasion is revealed by a series of trajectory snapshots during the simulation, shown in Figure 1. The absorption induces the headgroup of lipids disordering, and a gap in the surface appears below the NP after ~7 ns. Along with the NP embedding into the membrane, the gap is enlarged into a hole. Finally, the NP is stabilized on the midplane of the bilayer. Interestingly, during the whole process of inclusion, no water molecules are observed to enter into the hydrophobic core of the bilayer (see Supporting Information, SI_3), indicating the inclusion does not compromise the membrane integrity. The result of inclusion is consistent with recent experiments,[9,14] showing that charge-neutral PAMAM dendrimer nanoparticles can adsorb into the supported lipid bilayers, the membrane is thickened, but no new holes are formed. Such behavior agrees with another computer simulation which is based on the self-consistent field/density functional theory.[14] In that simulation, the neutral particle also entraps into the hydrophobic core of lipid bilayer. The final configurations of our simulation have supported, to some extent, their presumptions that for large neutral particles the membrane conformation remains intact rather than broken.

It is the local lipid integration/dissociation caused by the inclusion that is directly responsible for the bilayer deformation. The perturbation is likely to lead to local lipids segregation, where shorter chains of lipid molecules that match the NP dimensions more closely would concentrate in the region adjacent to the NP boundary. As a result, on the extracellular side, lipids are further divided into two categories: local (those adjacent to the NP) and bulk (all others) lipids. For a membrane that contains rigid inclusions, lipid molecules rearrange to optimize the membrane-inclusion interaction. And the rigid inclusion induces an asymmetry in the distribution of lipid molecules, known as hydrophobic mismatch.[25] Hydrophobic mismatching affects the global bilayer properties such as bilayer thickness, etc. The extent of hydrophobic mismatching in the simulation is visualized in Figure 2. Since the diameter of the spherical NP is larger than the average thickness of the lipid bilayer, the inclusion induces a positive hydrophobic mismatching[26] that the thickness of local lipids around the inclusion is larger than the average thickness of the lipid bilayer. In the simulation, close to the NP the membrane thickness is ~6.3 nm, about 53.6% larger than the average thickness of 4.1 nm of pure lipid bilayers. Depending on the rigidity of the lipids, at a distance from the NP the membrane thickness returns to normal. Adjacent to the NP the thickness has changed significantly, and the difference has vanished at about 2.5 nm from the NP center in our simulation. This value coheres with another theoretical result, which predicts that a hydrophobic inclusion can thicken the bilayer for distances of up to 2 nm from the inclusion.[27]

The lipids in cell membranes are in a disordered liquid state,[28] meaning that the NP adsorption and invasion induce the membrane deformation with ease. So, subsequent energy gain or loss due to the NP-induced deformation must be taken into account. We go on to address how the free energy changes as a function of the distance between the NP and the membrane. Such free energy surface is known as a potential of mean force (PMF).[29] Since the NP model is a solid sphere model, we can regard it as a rigid body which hardly undergoes conformation transitions. The free energy changes of inclusion mainly come from the NP−biomembrane coupling.

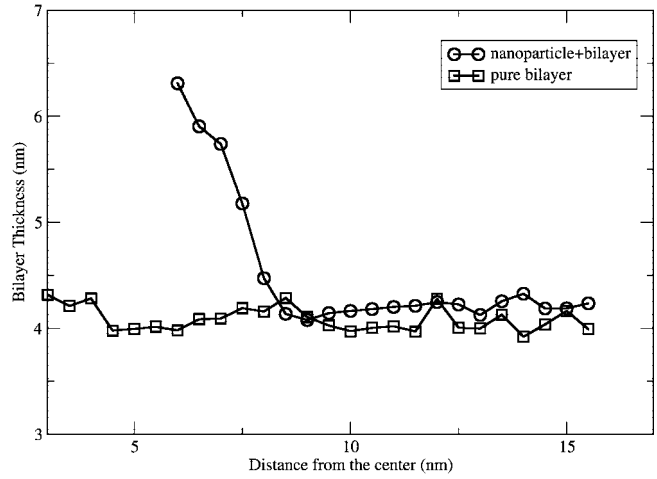

Figure 2. Altered membrane thickness around the embedded nanoparticle. The membrane thickness is measured in concentric rings around the NP center, depending on the distance to the center.

Here, we performed additional simulations to compute the PMF profile during the invasion of the hydrophobic NP. The free energy profile is calculated by means of the umbrella sampling technique[30] and the weighted histogram analysis method,[29] as follows:

$$W(\xi) = W(\xi^*) - k_B T \ln\left[\frac{\langle \rho(\xi) \rangle}{\langle \rho(\xi^*) \rangle}\right] \quad (1)$$

where W represents the function of PMF which is along some coordinate ξ, ξ^* and $W(\xi^*)$ are constants, k_B is the Boltzmann constant, and T is temperature.

Figure 3 shows the PMF of the hydrophobic NP as a function of its distance from the midplane of the DPPC bilayer. In addition, a local minimum of PMF is observed outside the bilayer at $z \sim -0.5$ nm, similar to the results that the PMF minimum is located at the bilayer center ($z \sim 0$ nm)[13] but somehow different from the results of Qiao et al. ($z \sim 1.1$ nm).[15] Moreover, around this position, the PMF profile changes mildly, rather than a comparatively severe change reported in studies mentioned above.

To obtain further understanding of this phenomenon, we consider that the PMF calculation undergoes the following processes: (I) the NP expelling lipid molecules to enter the hydrophobic core of the lipid bilayer, (II) lipid molecules accommodating the inclusion and rearranging, and (III) the NP inserting into the vacancy. In step I, the embedding behavior need to repulse the hydrophilic headgroups of lipids, leading to a significant cost in energy. However, the embedding NP is also driven by hydrophobic interactions of NP−water and NP−lipid tails, which enables its translocation across the headgroup of the bilayer. Step II also involves a gain in energy due to the interaction between the inserted NP and its surroundings lipids. For a large object inclusion, the local microscopic perturbation of the membrane shape around the inclusion becomes energetically unfavorable.[19] Thus, the membrane shape

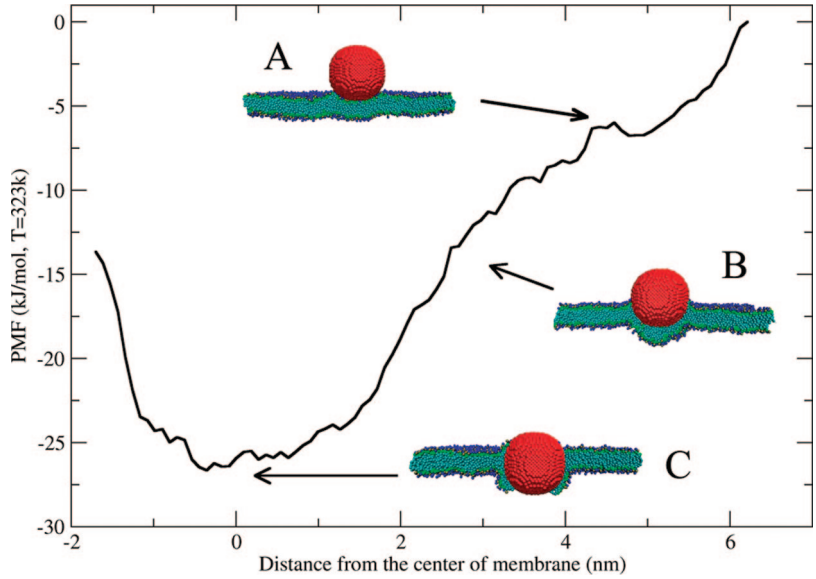

Figure 3. PMF of the hydrophobic NP as a function of its distance from the midplane of the DPPC bilayer, estimated with 88 sampling windows at a force constant of 27 000 kJ mol^{-1} nm^{-2}. Inset images (A−C) are snapshots corresponding to the sampling positions pointed by arrows.

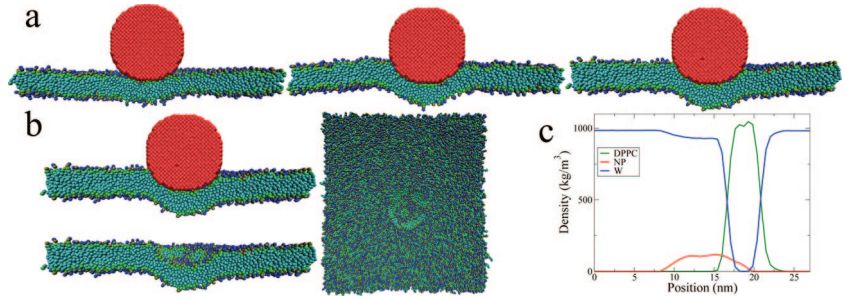

Figure 4. Trajectory snapshots of semihydrophilic NP simulation in stereo views: (a) different stages of the simulation process, (b) the final configuration of adsorption, (c) density profiles for different components of the final configuration.

remains locally unperturbed, and lipid molecules must rearrange to accommodate the inclusion. Correspondingly, the membrane adjusts to the shape of the inclusion through some lipid tilts deformation.[25] Step III is similar as step II, only the process is going on with a milder manner. The NP has penetrated the bilayer at step II, and both of its ends expose in the water during step III. The NP is forced to adjust its position by coaction of water and lipids molecules and stabilized at the final position.

For $z \sim 0$ nm situation reported by Marrink,[13] a hydrophobic sphere is modeled as a single Lennard-Jones atom with interaction parameter the same as that of the oxygen atom; the stable position in the simulation rests on van der Waals interactions between the sphere and its surrounding lipids.[15] For $z \sim 1.1$ nm situation reported in ref 15, the simulations employ a more realistic nanoparticle model, that a buckyball is explicitly modeled with 60 atoms, and the simulations also have considered some more complicated conditions, such as the difference of energy gain at these positions.[15] However, in all of these studies, the size of the hydrophobic NP is smaller than the thickness of the biomembrane. The fluctuation of lipid tails greatly influents the location of the NP. In our simulations, the diameter of NP is larger than the thickness of the bilayer; therefore, the fluctuation of lipid molecules results in less impact on the final position of the nanoparticle.[25] Though the NP is steady at the position of $z \sim -0.5$ nm in our simulation, the gently changing bottom of the PMF profile may imply that it is possible that the NP can be stable around the midplane of the bilayer. Also, the result may show the size effect exists during the inclusion of an external object. The relative importance of the physical mechanism discussed here remains to be elucidated in the future.

Simulations of Semihydrophilic Nanoparticles. In the simulation of the semihydrophilic nanoparticle, we observe that once the NP adsorbs on the surface of the lipid bilayer, it remains there except for some small fluctuations and does not move into the core of lipids during the simulation. Figure 4 shows the trajectory snapshots of the semihydrophilic NP−bilayer interaction. However, as some experimental studies have reported, a hydrophilic nanoparticle can enter into the cell via an endocytosis mechanism, that the nanoparticle is found to be wrapped in a lipid vesicle for the cell transportions.[18,31] Seeing that we may not observe this kind of transport mechanism due to the time limitation of the simulation, we also calculate the PMF profile of those situations that have not happened spontaneously in the simulation after the NP adsorbing on the bilayer. By the PMF profile, we want to know whether, from the perspective of energy, there is any probability that a semihydrophilic NP could be wrapped by the lipid bilayer. The PMF profile in Figure 5 explains the tendency for the semihydrophilic NP to remain on the surface of lipid membrane instead of moving toward the bilayer interior. After adsorption, the PMF increases with the distance decreases between the NP and the bilayer. The insets of Figure 5 show snapshots of the system configuration. The lipid bilayer in inset D has already deformed to wrap the NP partly. Note that when lipid bilayer deforms dramatically, the mass center of the membrane no longer stays at the midplane of the bilayer. The increasing PMF profile indicates there is a mere probability that a wrapping behavior

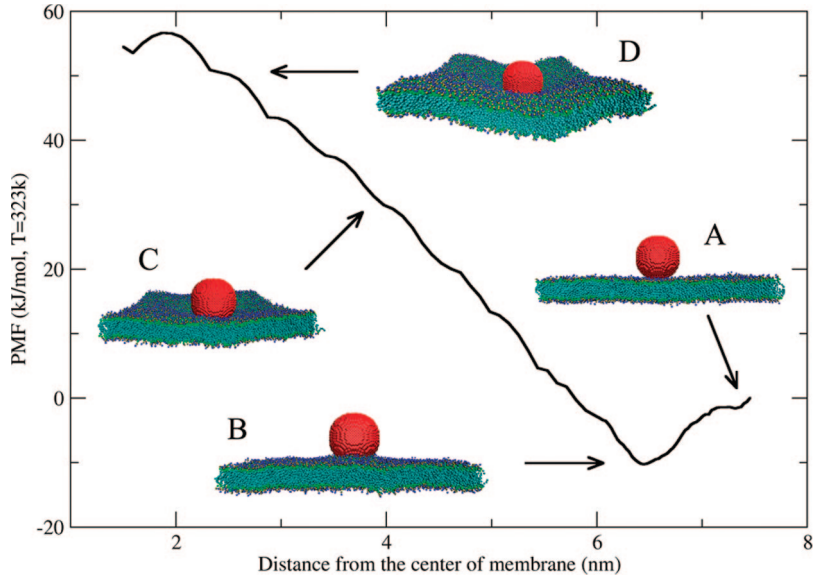

Figure 5. PMF of the semihydrophilic NP as a function of its distance from the midplane of the DPPC bilayer, estimated with 40 sampling windows at a force constant of 27 000 kJ mol^{-1} nm^{-2}. Inset images (A−D) are snapshots corresponding to the sampling positions pointed by arrows.

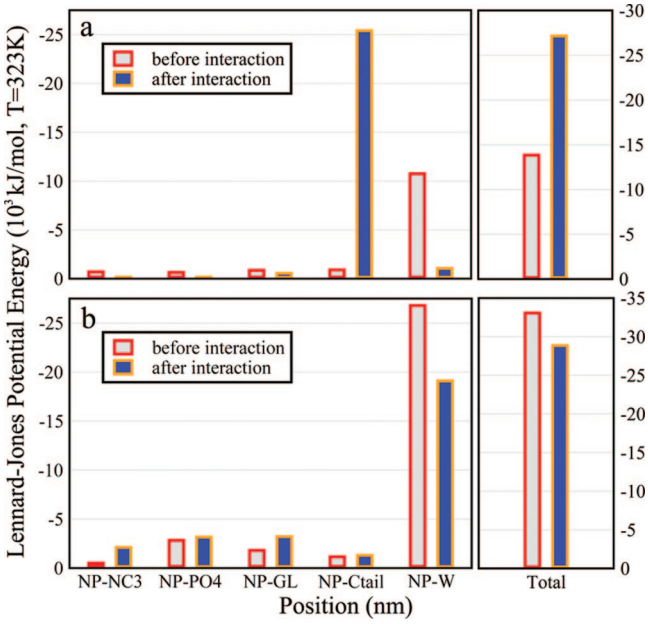

Figure 6. LJ potential energy contributions of different components in the interactions: (a) a hydrophobic NP case, (b) a semihydrophilic NP case.

occurs in our simulation because the wrapping behavior need to overcome a potentially substantial energy barrier. This result agrees with those results of some experiments, indicating that the endocytosis mechanism of cell is an energy-mediated process,[31] and some special proteins are need to assist the biomembrane in finishing the wrapping behavior.[32,33] This PMF profile is in agreement with Deserno's results of wrapping of a spherical colloid, which is obtained from the theoretical study within the framework of a Helfrich energy.[21] Those results are also proved in experiments, where gold nanoparticles coated by hydrophilic materials can hardly transport passively artificial phospholipid membranes.[34]

IV. Analysis of Thermodynamic Energy and Fluctuations

Some interesting hydrophobic effect has been reported, that some hydrophobic solutes translocation into ordered phases such as lipids differs from usual hydrophobic inversions.[35,36] Here, we give some analysis of the potential energy landscape of NP−biomembrane interactions for elucidating hydrophobicity differences. The interaction of NPs with the membrane through noncovalent forces includes van der Waals forces that are short-range attractive forces and electrostatic long-range interactions. In view of the electroneutrality of the NP model used in our simulations, the main energy contribution to the interaction is van der Waals forces, which is represented by the Lennard-Jones (LJ) potential. This LJ energy can be split further into five different contributions for the five different types of pair interactions between NP and other components of water and lipids. And this interaction energy can be calculated as the average over the simulated trajectory. Figure 6 shows these LJ potential energy contributions of different components in both NP−membrane interactions. The LJ potential energy of the hydrophobic NP−bilayer system decreases, whereas the energy increases in the semihydrophilic case. Since these unbiased simulations demonstrated favorable interactions between the NP and the lipids, both of processes are favorable by free energy (shown in Figures 3 and 5). It is not clear whether or not interactions are entropically favorable.

Another important issue addressed here is the membrane fluctuations induced by the NP interactions. In terms of both inclusion and adsorption, both behaviors of NPs can affect some macroscopic properties, such as surface tension of the biomembrane and also can result in the morphological changing of the biomembrane. Those changes associate with some biological behaviors of the biomembrane, such as budding and fission.[37] However, since the potential energy profiles show the transition in simulations undergoes a changing, nonequilibrium process, it seems merely possible to measure a macroscopic property of the system directly until the simulations really go into an equilibrium state. Here, a microscopic term local lipid density can be introduced to reflect the membrane fluctuation. For frames in the simulation trajectory, we split up the membrane into some concentric ring slices around the NP (see Supporting Information, SI_4), and local lipid density can be defined as

$$\text{density\_local} = \text{number\_lipid/area\_slice} \quad (2)$$

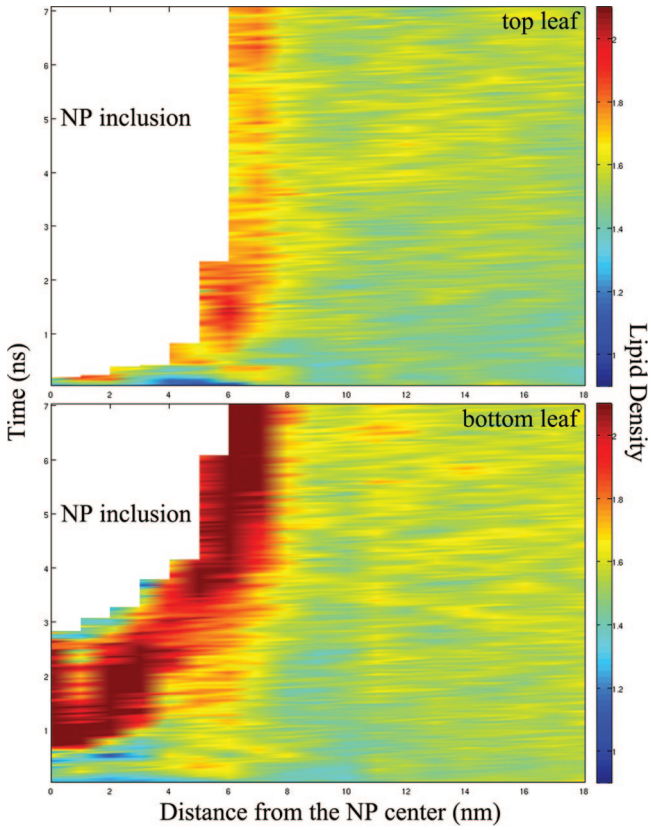

Figure 7. Local lipid density distribution in the hydrophobic NP interaction with lipids. The blank part in the image represents the NP inclusion into the membrane. The discontinuity left side of the landscape results from the reduced discrete sampling regions close to NP.

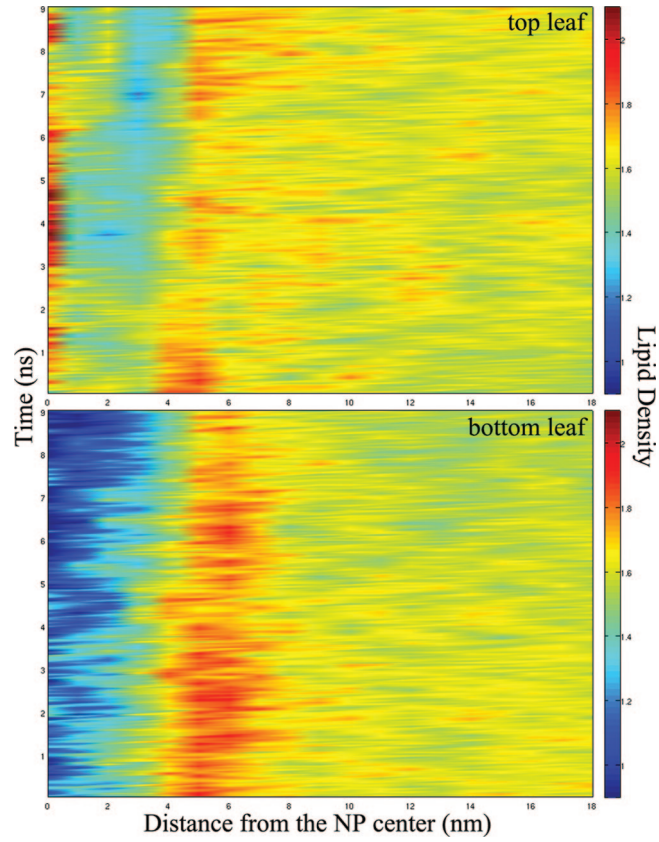

Figure 8. Local lipid density distribution in the semihydrophilic NP interaction with lipids.

where density_local represents the local lipid density, number_lipid the lipid number in the slice region, and area_slice the ring slice's area. The density should be calculated within some restrictions for simplicity: (1) the area is defined as the normal projected area; (2) in the hydrophobic NP case, the inclusion may induce segregations of the lipids within the interaction area from those surrounding lipids, so those lipids in the region are no more considered for the hydrophobic NP case once the NP contacting the top leaf. For two lipid leaves in a membrane patch, we define further one lipid leaf as top leaf, which nears the NP relatively in the initial configuration, whereas the other as bottom leaf. And the local lipid density landscapes of two leaves have been given respectively to distinguish different stages of interactions. Figure 7 shows the local lipid density variations of the hydrophobic NP case and Figure 8 for the semihydrophilic NP case.

The lipid density variations of the membrane have been obtained to reflect the fluctuations in the transition qualitatively. Different from those foregoing macroscopic results, local lipid density fluctuations give an expression of the microscopic variations of the lipids during the transitions. It is clear from the density landscapes that the deformation of the lipid bilayer due to the addition of the NP is short-range; those lipids adjacent to the NP are severely affected, whereas the others in the bulk are hardly sensitive to the interaction although there are still some small fluctuations in these regions. During the transition, the rearrangement of lipid molecules plays a significant role for an optimal adaptation to the addition of NPs. The landscape's differences between the top leaf and the bottom leaf have been seen for a membrane patch. These imply that, in the microscopic view of the thickness of the membrane not being omitted, two leaves of the membrane undergo different processes even at a same stage. As the result, the interaction makes the local lipid density changing within the adjacent region to the NP, corresponding to those situations of the hydrophobic mismatch in the hydrophobic NP case and partial wraps in the semihydrophilic NP case. Moreover, the density landscapes also reproduce the foregoing results for the hydrophobic NP case that the affected region vanishes at the distance of ~2.5 nm from the center. Anyhow, the additions of NPs are available to affect the lipid bilayer properties such as morphology, local lipid density, etc. Membrane is a self-assembly structure that brings about its adaptation to an external influence. All of these provide an interesting counterbalance to the tendency of the NP−biomembrane interaction.

V. Conclusion

With coarse-grained molecular dynamics simulations, the different mechanisms of NP−biomembrane interactions, due to the hydrophobicity of NPs, have been demonstrated. Two kinds of nanoparticles are considered in our simulations: one is hydrophobic and the other is semihydrophilic. In the former case, the nanoparticle embeds into the hydrophobic core of the membrane. The resulting lateral distribution of lipids around the inclusion is usually nonhomogeneous, known as hydrophobic mismatch. The results of no water being observed to enter into the core of bilayer implicate that charge-neutral NPs with surface hydrophobic functionalization don't result in the membrane leakage. In the latter case, the semihydrophilic effect of nanoparticle results in a different mechanism from the hydrophobic case, favoring the adsorption of NP on the surface of the bilayer rather than inclusion into the core. Spontaneous

wrapping action of the semihydrophilic NP by the membrane is not observed because of a potentially substantial energy barrier need to be overcome for finishing the wrapping process. The result shows indirectly that a cellular endocytosis-like uptake of NP is mediated through an energy-dependent mechanism. Moreover, for different system the local lipid density landscapes are obtained to reflect the membrane fluctuation in the simulations. These relevant results indicate that the deformation of the lipid bilayer is short-range, and the rearrangement of lipid molecules plays a significant role for the morphological variations of NP-containing lipid membrane patches. Those results could be applied in the design of specific nanoparticles for various biomedical applications.

Acknowledgment. We gratefully acknowledge the support to this research from the National Natural Science Foundation of China for financial support of this research (Grants 90406023 and 90406024) and the National Important Basic Research Program of China (Grants 2006CB933206 and 2006CB705606).

Supporting Information Available: Equilibrated configuration of the NP−water system and the equilibrated configuration of the hydrophobic NP−bilayer system. This material is available free of charge via the Internet at http://pubs.acs.org.

References and Notes

(1) Nel, A.; Xia, T.; Madler, L.; Li, N. *Science* **2006**, *311*, 622–627.
(2) Oberdorster, G.; Oberdorster, E.; Oberdorster, J. *Environ. Health Perspect.* **2005**, *113*, 823–839.
(3) Jung, T.; Kamm, W.; Breitenbach, A.; Kaiserling, E.; Xiao, J. X.; Kissel, T. *Eur. J. Pharm. Biopharm.* **2000**, *50*, 147–160.
(4) Joguparthi, V.; Xiang, T. X.; Anderson, B. D. *J. Pharm. Sci.* **2008**, *97*, 400–420.
(5) Gopalakrishnan, G.; Danelon, C.; Izewska, P.; Prummer, M.; Bolinger, P. Y.; Geissbuhler, I.; Demurtas, D.; Dubochet, J.; Vogel, H. *Angew. Chem., Int. Ed.* **2006**, *45*, 5478–5483.
(6) Zhang, L. F.; Hong, L.; Yu, Y.; Bae, S. C.; Granick, S. *J. Am. Chem. Soc.* **2006**, *128*, 9026–9027.
(7) Haryono, A.; Binder, W. H. *Small* **2006**, *2*, 600–611.
(8) Binder, W. H.; Sachsenhofer, R.; Farnik, D.; Blaas, D. *Phys. Chem. Chem. Phys.* **2007**, *9*, 6435–6441.
(9) Hong, S. P.; Bielinska, A. U.; Mecke, A.; Keszler, B.; Beals, J. L.; Shi, X. Y.; Balogh, L.; Orr, B. G.; Baker, J. R.; Holl, M. M. B. *Bioconjugate Chem.* **2004**, *15*, 774–782.
(10) Roiter, Y.; Ornatska, M.; Rammohan, A. R.; Balakrishnan, J.; Heine, D. R.; Minko, S. *Nano Lett.* **2008**, *8*, 941–944.
(11) Lee, A. G. *Biochim. Biophys. Acta* **2003**, *1612*, 1–40.
(12) Lee, J. H.; Lee, S. J.; Khang, G.; Lee, H. B. *J. Biomater. Sci., Polym. Ed.* **1999**, *10*, 283–294.
(13) Marrink, S. J.; Berendsen, H. J. C. *J. Phys. Chem.* **1996**, *100*, 16729–16738.
(14) Ginzburg, V. V.; Balijepailli, S. *Nano Lett.* **2007**, *7*, 3716–3722.
(15) Qiao, R.; Roberts, A. P.; Mount, A. S.; Klaine, S. J.; Ke, P. C. *Nano Lett.* **2007**, *7*, 614–619.
(16) Kessel, A.; Shental-Bechor, D.; Haliloglu, T.; Ben-Tal, N. *Biophys. J.* **2003**, *85*, 3431–3444.
(17) Lee, H.; Larson, R. G. *J. Phys. Chem. B* **2006**, *110*, 18204–18211.
(18) Chithrani, B. D.; Ghazani, A. A.; Chan, W. C. W. *Nano Lett.* **2006**, *6*, 662–668.
(19) Fosnaric, M.; Iglic, A.; May, S. *Phys. Rev. E* **2006**, *74*, 051503.
(20) Fosnaric, M.; Kralj-Iglic, V.; Bohinc, K.; Iglic, A.; May, S. *J. Phys. Chem. B* **2003**, *107*, 12519–12526.
(21) Deserno, M.; Bickel, T. *Europhys. Lett.* **2003**, *62*, 767–773.
(22) Marrink, S. J.; de Vries, A. H.; Mark, A. E. *J. Phys. Chem. B* **2004**, *108*, 750–760.
(23) Berendsen, H. J. C.; Postma, J. P. M.; Gunsteren, W. F. v.; DiNola, A.; Haak, J. R. *J. Chem. Phys.* **1984**, *81*, 3684–3690.
(24) Lindahl, E.; Hess, B.; van der Spoel, D. *J. Mol. Model.* **2001**, *7*, 306–317.
(25) May, S. *Curr. Opin. Colloid Interface Sci.* **2000**, *5*, 244–249.
(26) Fattal, D. R.; Ben-Shaul, A. *Biophys. J.* **1993**, *65*, 1795–1809.
(27) May, S. *Langmuir* **2002**, *18*, 6356–6364.
(28) Nagle, J. F.; Tristram-Nagle, S. *Biochim. Biophys. Acta* **2000**, *1469*, 159–195.
(29) Roux, B. *Comput. Phys. Commun.* **1995**, *91*, 275–282.
(30) Torrie, G. M.; Valleau, J. P. *Chem. Phys. Lett.* **1974**, *28*, 578–581.
(31) Rejman, J.; Oberle, V.; Zuhorn, I. S.; Hoekstra, D. *Biochem. J.* **2004**, *377*, 159–169.
(32) McMahon, H. T.; Gallop, J. L. *Nature (London)* **2005**, *438*, 590–596.
(33) Peter, B. J.; Kent, H. M.; Mills, I. G.; Vallis, Y.; Butler, P. J. G.; Evans, P. R.; McMahon, H. T. *Science* **2004**, *303*, 495–499.
(34) Banerji, S. K.; Hayes, M. A. *Langmuir* **2007**, *23*, 3305–3313.
(35) DeVido, D. R.; Dorsey, J. G.; Chan, H. S.; Dill, K. A. *J. Phys. Chem. B* **1998**, *102*, 7272–7279.
(36) MacCallum, J. L.; Tieleman, D. P. *J. Am. Chem. Soc.* **2006**, *128*, 125–130.
(37) Bickel, T. *J. Chem. Phys.* **2003**, *118*, 8960–8968.
(38) Humphrey, W.; Dalke, A.; Schulten, K. *J. Mol. Graphics* **1996**, *14*, 33–38.

JP8051906